Intranasal administration of convalescent plasma protects against SARS-CoV-2 infection in hamsters

Elise Wouters,[a,g] Caro Verbrugghe,[a,c,g] Rana Abdelnabi,[b] Rosalie Devloo,[a] Dorien De Clippel,[d] Dirk Jochmans,[b] Dominique De Bleser,[e] Birgit Weynand,[f] Veerle Compernolle,[a,c,d,e] Johan Neyts,[b] and Hendrik B. Feys[a,c,d,*]

[a]Transfusion Research Center, Belgian Red Cross-Flanders, Ghent, Belgium
[b]KU Leuven Department of Microbiology, Immunology and Transplantation, Rega Institute for Medical Research, Laboratory of Virology and Chemotherapy, B-3000, Leuven, Belgium
[c]Faculty of Medicine and Health Sciences, Ghent University, Ghent, Belgium
[d]Blood Services of the Belgian Red Cross-Flanders, Mechelen, Belgium
[e]Transfusion Innovation Center, Belgian Red Cross-Flanders, Ghent, Belgium
[f]KU Leuven Department of Imaging and Pathology, Translational Cell and Tissue Research, Division of Translational Cell and Tissue Research, B-3000, Leuven, Belgium

eBioMedicine
2023;92: 104597
Published Online 4 May 2023
https://doi.org/10.1016/j.ebiom.2023.104597

Summary

Background Convalescent plasma (CP) transfusion is an early option for treating infections with pandemic potential, often preceding vaccine or antiviral drug rollout. Heterogenous findings from randomized clinical trials on transfusion of COVID-19 CP (CCP) have been reported. However, meta-analysis suggests that transfusion of high titer CCP is associated with a mortality benefit for COVID-19 outpatients or inpatients treated within 5 days after symptom onset, indicating the importance of early administration.

Methods We tested if CCP is an effective prophylactic against SARS-CoV-2 infection by the intranasal administration of 25 µL CCP/nostril (i.e. 0.01–0.06 mg anti-RBD antibodies/kg) in hamsters exposed to infected littermates.

Findings In this model, 40% of CCP treated hamsters were fully protected and 40% had significantly reduced viral loads, the remaining 20% was not protected. The effect seems dose-dependent because high-titer CCP from a vaccinated donor was more effective than low-titer CCP from a donation prior to vaccine rollout. Intranasal administration of human CCP resulted in a reactive (immune) response in hamster lungs, however this was not observed upon administration of hamster CCP.

Interpretation We conclude that CCP is an effective prophylactic when used directly at the site of primary infection. This option should be considered in future prepandemic preparedness plans.

Funding Flanders Innovation & Entrepreneurship (VLAIO) and the Foundation for Scientific Research of the Belgian Red Cross Flanders.

Keywords: COVID-19; SARS-CoV-2; Convalescent plasma; Prophylaxis; Intranasal

Introduction

The COVID-19 pandemic is the deadliest in recent history. Outbreaks of communicable diseases are inevitable following increased interactions of humans with wildlife.[1,2] Pandemic preparedness therefore implies continuous investment on several fronts. Strategic stockpiling of highly potent and safe antivirals against (entire families of) viruses with known epidemic and pandemic potential is one. Novel vaccines and vaccine platforms like mRNA technology is another. However, major investments in broad spectrum antivirals and quick vaccine rollout plans do not guarantee the next bug being beaten at first inning. Clinical trials take time and success of treatment is not always certain as the Ebola and HIV crises showed.[3] Consequently, an 'early transitional phase option' that bridges the start of the epidemic and the rollout of successful clinical treatments is still needed in global pandemic preparedness plans.

One of the first available products with antiviral potential during an epidemic is convalescent plasma (CP).

DOI of original article: https://doi.org/10.1016/j.ebiom.2023.104626
*Corresponding author. Transfusion Research Center, Belgian Red Cross-Flanders, Ghent, Belgium.
E-mail address: hendrik.feys@rodekruis.be (H.B. Feys).
[g]These authors contributed equally.

Research in context

Evidence before this study

COVID-19 convalescent plasma (CCP) is collected from recovered COVID-19 patients and contains anti-SARS-CoV-2 antibodies. CCP transfusion has been tested extensively during the COVID-19 pandemic but might only be effective in a general population of hospitalized patients when treated early on in the disease course. Typically, CCP transfusion dilutes the anti-SARS-CoV-2 antibodies by a factor 10 or more which may be one reason why it is ineffective in this population. Furthermore, it is unclear if CCP antibodies effectively reach the naso- and oropharyngeal mucosa where primary infection is taking place.

Added value of this study

Our data demonstrate that CCP can be applied intranasally where it protects against viral transmission in hamsters exposed to SARS-CoV-2 infected littermates.

Implications of all the available evidence

Novel viruses will keep emerging and the scientific community will react with novel vaccines and antivirals. But these take time to develop, even at the unprecedented rates of recent times. There is currently nothing to bridge that particular lapse between identification of the novel virus and the rollout of effective drugs or vaccines. Our study suggests that a nasal spray filled with CCP may protect against virus transmission of SARS-CoV-2 and warrants further study in humans.

It is inexpensive and can be made available relatively quickly. COVID-19 convalescent plasma (CCP) transfusion was used within one month after the first SARS-CoV-2 report.[4] But randomized clinical trials (RCTs) then reported heterogenous findings on the efficacy of CCP transfusion in COVID-19 hospitalized patients.[5–9] CCP transfusion may however be efficacious as suggested by meta-analysis of multiple RCTs, particularly in (immunocompromised) patients that are treated early in the course of infection and using high titer CCP.[10–16]

Historically, CP has only been used as transfusion therapy. However, transfusion inevitably dilutes CP donor antibodies to 6–12% using a typical volume of 300 and 600 mL in an average patient with a blood volume of 5 L. In addition, in infections like COVID-19 or influenza these diluted donor antibodies have to cross endothelial and epithelial barriers to reach peripheral sites of infection. In the case of SARS-CoV-2 the primary site of infection is the naso- and oropharyngeal mucosa[17–20] and it is unclear if antibodies easily reach these tissues in time and in sufficient and effective quantities following transfusion.

Therefore, we hypothesized that direct application of CCP or CCP from a vaccinated donor to the primary site of infection using intranasal (i.n.) administration can prevent or attenuate SARS-CoV-2 transmission. To model this, we used a Syrian hamster model of virus transmission and demonstrated that this is indeed possible.

Methods

Samples

Plasma was collected by plasmapheresis from a SARS-CoV-2 recovered donor (January 2021) or from a vaccinated SARS-CoV-2 recovered donor (January 2022). This material will be referred to as COVID-19 convalescent plasma (CCP) and vaccinated COVID-19 convalescent plasma (VCCP), respectively. The neutralizing titer of the convalescent donations was determined by plaque reduction neutralizing test (PRNT) at least 14 days after resolution of symptoms. The VCCP was collected after confirmation of a high (neutralizing) antibody titer in enzyme-linked immunosorbent assays (ELISA) 1 month after the booster vaccine and at 18 days after resolution of symptoms. The VCCP donor received a Pfizer/BioNTech (Comirnaty) vaccine and a booster vaccine of Moderna (Spikevax). Plasma collected from a single donor from before the pandemic was used as naive, non-immune control (NIP_{HUMAN}). Signed, informed consent was obtained from all donors. Samples used for scientific research were registered by the Belgian Red Cross Flanders biobank (BB190034). The activities of the biobank are approved by the University Hospital KU Leuven Institutional Review Board (S62549).

Pooled non-immune hamster plasma ($NIP_{HAMSTER}$) was provided by Janvier Labs (Le Genest-Saint-Isle, France) and by the Rega Institute (KU Leuven, Belgium). Convalescent hamster plasma ($CCP_{HAMSTER}$) was retrieved from Innovative Research (Pearl Court Novi, USA).

The immunoglobulin fraction from the VCCP sample (hIg) was purified by affinity chromatography using protein A (ab270308, Abcam) and G resin (ab270309, Abcam) according to the manufacturer's instructions. hIg was dialysed to phosphate buffered saline (PBS), pH 7.4. A fraction was lyophilized and reconstituted in $NIP_{HAMSTER}$.

In vitro characterization of human plasma samples

Plates were coated overnight with recombinant receptor binding domain (RBD) at 1 μg/mL (YP_009724390.1) (Arg319-Phe541) (40592-V08H, Sino Biological). Plates were blocked with PBS and 1% [wt/vol] bovine serum albumin (BSA) (assay buffer) for the IgG isotype ELISA or PBS with 5% [vol/vol] rabbit serum for IgA and IgM. Plasma was diluted in assay buffer as follows; NIP_{HUMAN} 1/200 (IgG ELISA), 15/100 (IgA ELISA) or 1/10 (IgM ELISA); CCP and hIg 1/2000 (IgG ELISA), 1.5/100 (IgA ELISA) or 1/10 (IgM ELISA); VCCP 1/2000 (IgG and IgA

ELISA) or 1/10 (IgM ELISA). Technical triplicates were performed. The WHO international standard (NIBSC number: 20/136) was included as a standard.[21] Bound antibodies were detected using rabbit anti-human secondary IgG (anti-Fc_{γ}, 1:15,000), IgA (anti-α chain, 1:10,000) or IgM (anti-$Fc_{5\mu}$, 1:10,000) (IgG: Cat # 309-035-008 and RRID: AB_2339649, IgA: Cat # 309-035-011 and RRID:AB_2339650, IgM: Cat # 309-035-095 and RRID:AB_2339654, Jackson ImmunoResearch). Intra- and inter-assay coefficient of variation (CV) was below 10 and 15% respectively for all isotype ELISAs (n = 5).

To determine antibody concentrations, a serial dilution of either anti-RBD human IgG_1 (srbd-mab1, Invivogen) or anti-RBD human IgA_1 (srbd-mab6, Invivogen) was used as a standard using a non-immune human plasma pool from 15 donors as diluent. Technical triplicates were performed. Intra- and inter-assay CV was below 15% and 20% respectively (n = 4).

The inhibition ELISA (EP-105, AcroBiosystems) was performed according to the manufacturer's instructions except for sample preparation. Briefly, RBD was coated overnight at 4 °C. Blocking was with 2% [wt/vol] BSA in PBS. An eight-step serial dilution of plasma in PBS with 0.5% [wt/vol] BSA was incubated with biotinylated recombinant angiotensin converting enzyme 2 (ACE2). Bound ACE2 was detected using streptavidin-HRP. Data were converted to the WHO standard.

Data was processed in GraphPad Prism version 9 (GraphPad Software Inc., San Diego, CA, USA). (Neutralizing) antibody levels were calibrated against the WHO standard and expressed as BAU/mL or international units per mL (IU/mL). The lower limit of detection (LOD) was 32 BAU/mL for the IgG isotype ELISA, 14 BAU/mL for the IgA isotype ELISA, 39 BAU/mL for the IgM isotype ELISA, 1.1 μg/mL for the IgG concentration ELISA, 0.2 μg/mL for the IgA concentration ELISA and 26 IU/mL for the inhibition ELISA.

Plaque reduction neutralization test (PRNT)

The PRNT was performed as previously described.[10,22] Variants used were SARS-CoV-2 ancestral strain (BetaCov/Belgium/GHB-03021/202, EPI ISL 407976|2020-02-03, passage 5),[23] Delta B.1.617.2 (hCoV-19/Belgium/rega-7214/2021; EPI_ISL_2425097, passage 2)[24,25] and Omicron B.1.1.529 (hCoV-19/Belgium/rega-20174/2021, EPI_ISL_6794907|2021, passage 2).[26] In brief, a ten-step serial dilution was prepared for samples CCP, VCCP and NIP_{HUMAN}. Dose-dependent neutralization was assessed by mixing the plasma dilutions with 100 plaque forming units (PFU) of a SARS-CoV-2 variant in Dulbecco's Modified Eagle's Medium (DMEM) with 2% [vol/vol] fetal bovine serum (FBS). These were added to VeroE6 cell monolayers (African green monkey kidney, RRID: CVCL_0574, ATCC CRL-1586) in 12-well plates. Next, the inoculum mixture was replaced with 0.8% [wt/vol] methylcellulose in DMEM with 2% [vol/vol] FBS. After three days at 37 °C the overlays were removed, cells were fixed with 3.7% [wt/vol] paraformaldehyde (PFA) and stained with 0.5% [wt/vol] crystal violet. The half-maximum neutralization titers ($PRNT_{50}$) were defined.

Animals

Wild type Syrian Golden hamsters (*Mesocricetus auratus*) were purchased from Janvier Laboratories. Specific-pathogen-free 6–8 weeks-old female hamsters were ear-tagged and allocated as pairs (i.e. without any selection criteria) into cages. No randomization method was used, nor confounders were controlled. However, all caretakers, technicians and the pathologist were blinded to treatment allocation in the animal facility and for analysis (qPCR, titration and histology). In addition, all hamsters were female, had the same age and roughly the same weight, indicating that no real confounding factor should be considered that may impact the outcome of the study.

Ethics statement

Housing conditions and experimental procedures were approved by the ethics committee of animal experimentation of KU Leuven (license P065-2020). Animals were housed in ventilated isolator cages (IsoCage N Biocontainment System, Tecniplast) at 21 °C, 55% humidity and 12:12 day/night cycles. Ad libitum access to food and water was supplied together with cage enrichment (wood block). Animals were acclimated four days prior to the start of the study.

Sample size

Animal group size was calculated using the G*Power 3.1.9.7 software (Heinrich-Heine-Universität Düsseldorf, Düsseldorf, Germany) with an independent T-test implementing an effect size of 2 (calculated based on at least 1 $\log_{10}$ reduction in viral RNA and/or $TCID_{50}$ levels), a significance level α of 0.05 and a power of 95%. This resulted in sample size of 6 animals/group, which is conform with the housing and handling capacity under BSL3 conditions at the Rega Institute.

SARS-CoV-2 transmission model in hamsters

The transmission model has been described before.[27] In brief, index hamsters were infected i.n. with 50 μL (25 μL/nostril) containing 2×10^6 $TCID_{50}$ SARS-CoV-2 (day 0) under anaesthesia with ketamine/xylazine/atropine. Virus titers were determined by Reed and Muench method.[28] Naive hamsters (sentinel) were assigned into different treatment groups and intranasally treated with 25 μL/nostril of any of the mentioned plasma samples without any preference. Each sentinel was then co-housed with a randomly assigned index infected hamster in ventilated cages.

Sentinels were treated i.n. under anaesthesia with isoflurane daily for 5 consecutive days with plasma but

starting 1 day prior to co-housing with the index hamster. Sentinels were treated with 25 µL/nostril of CCP (n = 18 over two independent experiments, 0.01 mg anti-RBD Ig/kg), VCCP (n = 6, 0.06 mg anti-RBD Ig/kg), hIg (n = 6, 0.05 mg anti-RBD Ig/kg), NIP_{HUMAN} (n = 6), $CCP_{HAMSTER}$ (n = 6), $NIP_{HAMSTER}$ (n = 6) and hIg in $NIP_{HAMSTER}$ (n = 6). As a negative control, sentinels were treated with PBS pH 7.4 (n = 14 over two independent experiments). All hamsters were monitored for appearance, behaviour and weight.

Sample collection

Index hamsters were sacrificed at day 4 post infection and sentinels at day 4 post co-housing. Hamsters were euthanized by intraperitoneal (i.p.) injection of 500 µL Dolethal (200 mg/mL sodium pentobarbital, Vétoquinol SA). Lung tissue was prepared for analysis as described previously.[27] Left lung lobes were collected for histopathological examination. Right lung lobes were collected for viral RNA and infectious virus quantification.

SARS-CoV-2 RT-qPCR has been described before.[27,29] Briefly, lung tissues were homogenized using bead disruption (Precellys) (E.Z.N.A.® Total RNA Kit, Omega Bio-tek). The cell debris was pelleted and RNA was extracted according to the manufacturer's instructions. Using the LightCycler96 platform (Roche Diagnostics, Rotkreuz, Switzerland) the nucleocapsid of SARS-CoV-2 was targeted with N2 primers and probes using the iTaq Universal Probes One-Step RT-qPCR kit (BioRad). Standards of SARS-CoV-2 cDNA (Integrated DNA Technologies, Iowa, USA) were used to express the amount of viral genome copies per mg tissue. A standard curve of Ct versus genome copies per mL was generated using 10-step dilutions of SARS-CoV-2 cDNA. Then, based on the eluted volume of the RNA extract the total number of genome copies was calculated. The number of genome copies was normalized against the weight of the lung tissue from which the RNA was extracted. No exclusions of data points in the analysis were made.

End-point virus titrations (TCID) have been described before.[27] In brief, lung tissues were homogenized using bead disruption (Precellys) in 350 µL minimal essential medium (MEM) and centrifuged at 10,000 g for 5 min. The infectious particles are quantified through endpoint titrations on confluent Vero E6 cells. Viral titers were calculated by the Reed and Meunch method.[28] The viral titer was expressed as 50% tissue culture infectious dose ($TCID_{50}$) per mg tissue.

For histological examination, lungs were fixed in 4% formaldehyde and embedded in paraffin.[27] Longitudinal tissue sections (5 µm) were analysed after haematoxylin and eosin (H&E) staining and scored for lung damage by an independent expert pathologist blinded from cohort information. The scored parameters, to which a score of 1–3 was attributed, were the following: congestion, intra-alveolar haemorrhage, apoptotic bodies in bronchus wall, perivascular oedema, bronchopneumonia, perivascular inflammation, peribronchial inflammation and vasculitis. The cumulative lung score represents the sum of the relevant scored parameters.

Statistics

Statistical significance between treatment groups was determined by GraphPad Prism 9 software (GraphPad, San Diego, CA, USA) using a non-parametric Kruskal–Wallis with Dunn's post hoc test. P-values of <0.05 were considered significant.

Role of funders

The Funders had no role in the study design, data collection, data analyses, interpretation or writing the report.

Results

Characterization of human (convalescent) plasma samples, *in vitro*

Four human samples were used to test our hypothesis; (1) convalescent plasma from a donor recovered from COVID-19 without vaccination (CCP), (2) convalescent plasma from a different donor recovered from COVID-19 and later vaccinated against SARS-CoV-2 (VCCP), (3) purified immunoglobulin fraction from VCCP (hIg) and (4) non-immune plasma donated before the pandemic (NIP_{HUMAN}).

VCCP contained 4-fold higher 'binding antibody units' (BAU)/mL levels of anti-RBD IgG and 13-fold higher BAU/mL levels of anti-RBD IgA compared to CCP (Fig. 1a and b) while anti-RBD IgM BAU/mL levels were near or below the detection limit of the assay in both samples (Fig. 1c). The anti-RBD IgG and anti-RBD IgA plasma concentration was in line with these BAU/mL levels (Fig. 1d and e). The three convalescent samples CCP, VCCP and hIg effectively inhibited RBD interaction with ACE2 *in vitro*, while NIP_{HUMAN} did not (Fig. 1f). Viral replication *in vitro* of the ancestral strain infecting Vero E6 cells was inhibited most by VCCP, followed by CCP and NIP_{HUMAN} (Fig. 1g). The purity and yield of neutralizing antibodies in hIg was assessed by SDS-PAGE with Coomassie staining and ELISA, respectively (Supplementary Fig. S1a and b). Total protein concentration in hIg was 14.8 mg/mL and anti-RBD IgG was 95 ± 14 µg/mL, yielding 0.6% anti-RBD IgG by protein mass fraction. The BAU/mL level of anti-RBD IgG in hIg was comparable to that in VCCP (Fig. 1a) while the BAU/mL level of anti-RBD IgA was 13-fold lower (Fig. 1b) having a concentration just above the detection limit of 0.2 µg/mL (Fig. 1e). Neutralization of delta and omicron virus variants by VCCP and CCP was significantly higher than control NIP_{HUMAN}, but was reduced compared to neutralization of the ancestral strain (Supplementary Fig. S2a and b & Fig. 1g).[30]

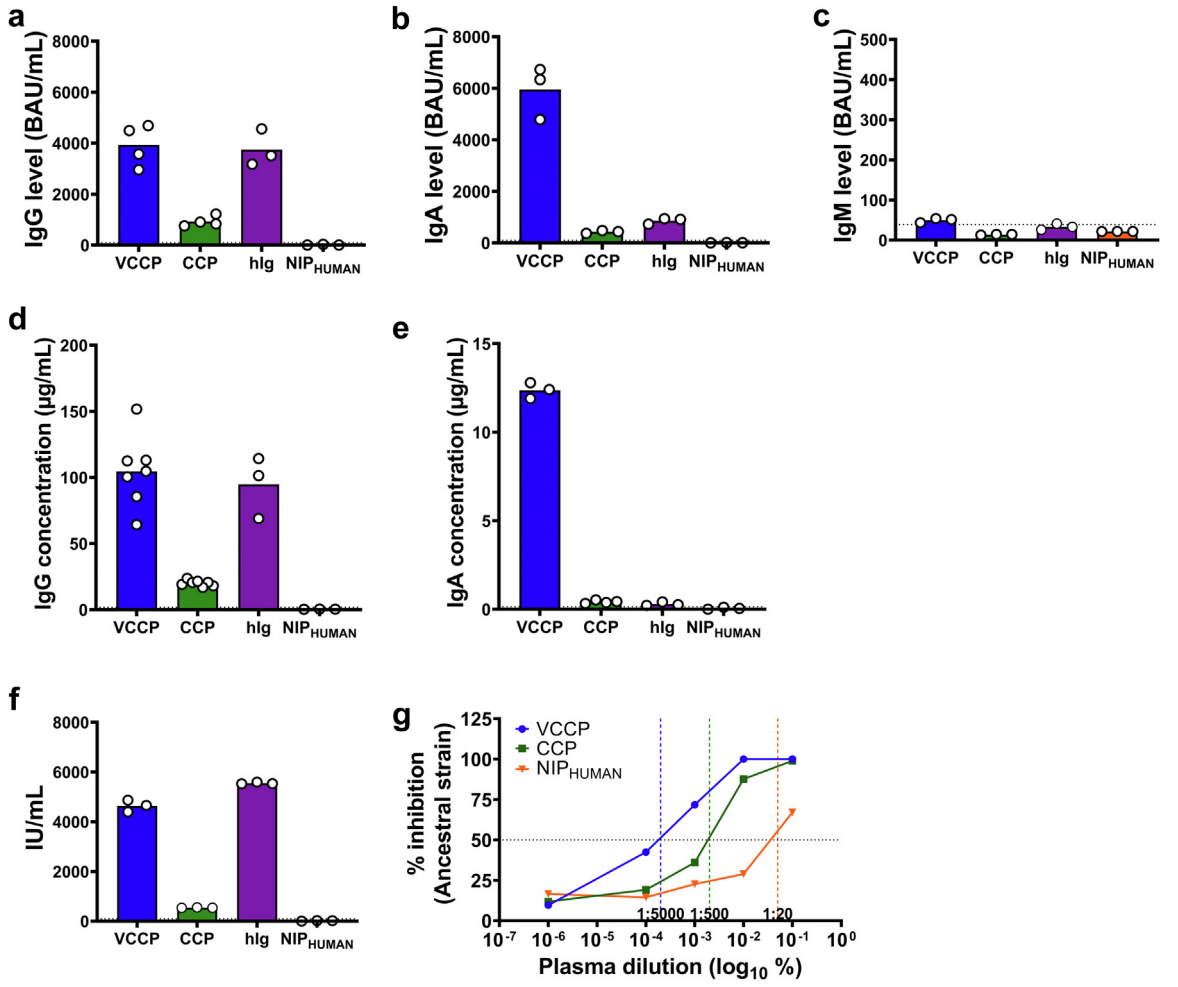

***Fig. 1: In vitro* characterization of the human (convalescent) plasma samples.** The antibody content, concentration and neutralizing capacity was determined in ELISA and by plaque reduction neutralization test. (**a-c**) The anti-RBD levels of IgG expressed in BAU/mL (**a**), IgA (**b**) and IgM (**c**). (**d-e**) The anti-RBD concentration of IgG (**d**) and IgA (**e**) given in µg/mL. (**f**) Inhibition of ACE2 binding to RBD by plasma and expressed as international WHO standard (IU/mL). In these panels (**a-f**) the horizontal dotted line represents the lower limit of detection. Bars represent mean and dots the individual data (technical repeats, n ≥ 3). (**g**) Inhibition of plaque formation in VeroE6 cultures infected with the ancestral SARS-CoV-2 strain. The horizontal dotted line at 50% inhibition is plotted to indicate the intersection with the inhibition data from the plasma samples to deduce the $PRNT_{50}$ values (*coloured dotted line*). Dots represent individual data (n = 1, in duplicate). Coloured lines indicate the serial dilution per sample.

Prophylaxis of SARS-CoV-2 transmission by i.n. administration of human convalescent samples

The study design is depicted in Fig. 2a. Sentinel hamsters were treated i.n. with human convalescent samples (containing dosages of anti-RBD Ig ranging from 0.01 mg/kg (CCP) to 0.06 mg/kg (VCCP)) for five consecutive days while co-housed with an infected untreated index hamster from day one. There were no signs of weight loss or toxicity during the experiment (Fig. 2b). At endpoint, viral RNA copies in the lungs of sentinel hamsters treated with VCCP, CCP and hIg were significantly reduced by $\log_{10}$ 2.1-, 2.4- and 2.5-fold respectively, compared to sentinel hamsters treated with buffer (Fig. 2c & Supplementary Table S1). Intranasal treatment with NIP_{HUMAN} did not reduce viral RNA compared to buffer (P = 0.6). In line with these data, infectious virus titers, expressed as tissue culture infectious dose ($TCID_{50}$)/mg lung were also significantly reduced by $\log_{10}$ 3.2-, 2.8- and 2.3-fold in sentinel hamsters treated with VCCP, CCP and hIg respectively, compared to sentinel hamsters treated with buffer (Fig. 2d & Supplementary Table S1). The decrease in infectious virus levels was highest in VCCP treated animals, suggesting a dose dependent relation between the anti-SARS-CoV-2 immunoglobulins in plasma and the effect. Taken together, detectable infectious virus (<1.5

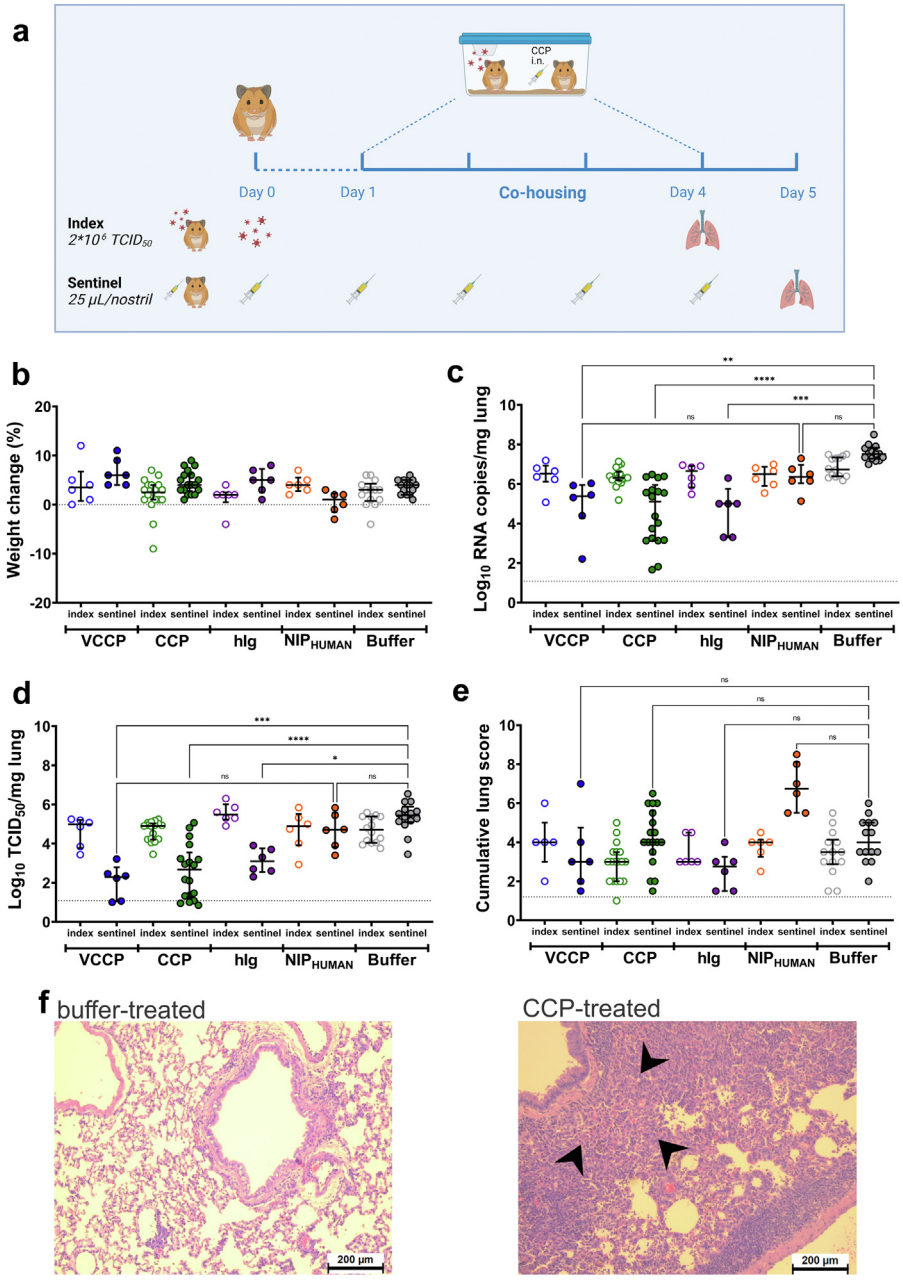

Fig. 2: **Intranasal administration of human (convalescent) plasma in hamsters as prophylaxis against SARS-CoV-2 transmission.** (**a**) The study design depicts sentinel hamsters treated daily from day 0 onwards with i.n. VCCP (n = 6), NIP_{HUMAN} (n = 6), hIg (n = 6), CCP (n = 18) or buffer (n = 14) and index hamsters inoculated at day 0 with SARS-CoV-2 ancestral strain. Animals were co-housed from day 1 until day 4. (**b**) The relative weight change (%) determined on the day of sacrifice and normalized to that on day 0. (**c**) Viral RNA levels in the lung measured by RT-qPCR and expressed as log_{10} RNA copies/mg lung tissue. (**d**) Infectious virus in lung homogenate expressed as log_{10} $TCID_{50}$/mg lung tissue. (**e**) Cumulative lung score as determined by histopathologic assessment of H&E prepared lung sections. (**b-e**) Individual dots represent biological repeats. The median (*horizontal line*) and interquartile range (*error bars*) are plotted. The horizontal dotted line represents the lower limit of detection. Statistical significance between cohorts was calculated by Kruskal–Wallis with Dunn's post hoc test. *P < 0.05, **P < 0.01, ***P < 0.001, ****P < 0.0001, ns = not significant. (**f**) A representative H&E-stained lung section taken from a sentinel hamster that was treated i.n. with buffer (*left*) or with CCP (*right*). The lungs of sentinel hamsters treated i.n. with CCP had obvious signs of pneumocyte hyperplasia (*butterfly arrow,* ➤). Microscopic image acquisition was at 100 magnification (200 µm *scale bar*), using a 10×/20 objective with 10×/0.22 NA and bright field settings.

log_{10} $TCID_{50}$/mg lung) was absent in the lungs of 2/6 (33%) sentinel hamsters treated with VCCP and 7/18 (39%) sentinel hamsters treated with CCP. A significant reduction in infectious virus (<3.5 log_{10} $TCID_{50}$/mg lung) was found in 4/6 (67%) sentinel hamsters treated with VCCP and 7/18 (39%) sentinel hamster treated with CCP.

These biological results did not corroborate with the clinical picture of the hamster lungs. Histology lung score of sentinel hamsters treated with VCCP, CCP and hIg was not different from sentinel hamsters treated with buffer (Fig. 2e & Supplementary Table S2) suggesting lung damage despite decreased infection. However, the nature of this lung damage in sentinel hamsters treated with VCCP, CCP and NIP_{HUMAN} was different from characteristic infectious inflammation caused by SARS-CoV-2 infection. Pneumocyte hyperplasia and intra-alveolar eosinophils suggested a reactive (immune) response linked to the treatment instead of infectious pneumonia causative of a viral infection (Fig. 2f, Supplementary Fig. S3a & Supplementary Table S2). This histopathologic picture was absent in index hamsters and in sentinel hamsters treated with buffer (Fig. 2f, Supplementary Fig. S3b & Supplementary Table S2).

Side effects in hamster lungs caused by i.n. administration of human versus hamster plasma

The histology data suggest that i.n. administration of human plasma causes an immune reaction in hamster lungs. To assess a potential species effect related to this reaction, plasma or serum from either human or hamster origin was administered i.n. for five days in the absence of viral challenge, followed by histopathology scoring (Fig. 3a). Control samples were hIg in buffer, hIg in non-immune hamster plasma ($NIP_{HAMSTER}$) and buffer. No weight loss or signs of toxicity were observed in the naive hamsters (Fig. 3b).

Lung scores were significantly increased following administration of NIP_{HUMAN} (n = 3) compared to buffer (n = 6) (P = 0.03) (Fig. 3c & Supplementary Table S3). A minor increase in the lung score was observed in hamsters treated with VCCP or serum and hIg in $NIP_{HAMSTER}$ (P > 0.10) (Fig. 3c & Supplementary Table S3). Animals treated with $NIP_{HAMSTER}$ or hamster serum had healthy lungs indistinguishable from control hamsters treated with buffer (P > 0.999) (Fig. 3c & Supplementary Table S3).

Pneumocyte hyperplasia was found in 10% of the assessed lung section in 2/3 of hamsters treated with NIP_{HUMAN} (Fig. 3d & Supplementary Table S3). Perivascular inflammation was found in all hamsters treated with NIP_{HUMAN}, hIg in $NIP_{HAMSTER}$ or VCCP and in 2/9 of hamsters treated with $NIP_{HAMSTER}$ (Fig. 3d & Supplementary Table S3). Perivascular oedema was mostly present in hamsters treated with NIP_{HUMAN} (2/3) and one case was observed in the hamsters treated with VCCP (1/6) and hIg in $NIP_{HAMSTER}$ (1/6) (Supplementary Table S3). Pneumocyte hyperplasia and perivascular oedema were absent in hamsters treated with $NIP_{HAMSTER}$ or hamster serum (Fig. 3d; Supplementary Table S3).

Prophylaxis of SARS-CoV-2 transmission by i.n. administration of hamster convalescent samples

To investigate if the prophylactic effect of i.n. convalescent plasma can be dissected from the reactive (immune) response caused by species incompatibility, COVID-19 convalescent plasma from hamsters ($CCP_{HAMSTER}$) was tested. Its effect was compared to $NIP_{HAMSTER}$ as well as to hIg in $NIP_{HAMSTER}$ and buffer. Both $CCP_{HAMSTER}$ and hIg in $NIP_{HAMSTER}$ significantly inhibited RBD binding to ACE2 *in vitro* compared to $NIP_{HAMSTER}$ alone (Fig. 4a).

The experimental model of virus transmission was the same as presented in Fig. 2a. Weight and vital signs remained at baseline in all cohorts during the course of study (Fig. 4b). As with human convalescent plasma, viral RNA genome copies in the lungs of sentinel hamsters treated with $CCP_{HAMSTER}$ or hIg in $NIP_{HAMSTER}$ were significantly reduced by a log_{10} 3.1 and 4.5-fold respectively, compared to sentinel hamsters treated with buffer (Fig. 4c & Supplementary Table S1). Infectious virus titers in sentinel hamsters treated with $CCP_{HAMSTER}$ or hIg in $NIP_{HAMSTER}$ were significantly reduced by a log_{10} 2.7- and 2.3-fold respectively, compared to buffer controls (Fig. 4d & Supplementary Table S1). Infectious virus was absent in 1/6 (17%) sentinel hamsters treated with $CCP_{HAMSTER}$ and in 2/6 (33.3%) sentinel hamsters treated hIg in $NIP_{HAMSTER}$. A significant reduction in infectious virus was observed in 3/6 (50%) sentinel hamsters treated with $CCP_{HAMSTER}$ and 4/6 (66.6%) sentinel hamsters treated with hIg in $NIP_{HAMSTER}$.

Histopathology scores in sentinel hamsters treated with $NIP_{HAMSTER}$ or hIg in $NIP_{HAMSTER}$ was above baseline and not different from buffer treated controls (P > 0.999) (Fig. 4e & Supplementary Table S4). This indicates lung damage by human protein and by viral infection, respectively. Lung scores of sentinel hamsters treated with $CCP_{HAMSTER}$ were at baseline, except in one animal with mild lung involvement. There were no signs of pneumocyte hyperplasia nor intra-alveolar eosinophils in lungs of sentinel hamsters treated with $CCP_{HAMSTER}$ (Fig. 4f, Supplementary Fig. S4a–c and Supplementary Table S4). In this experiment, hamsters treated with hIg in $NIP_{HAMSTER}$ or with $NIP_{HAMSTER}$ did not present pneumocyte hyperplasia nor intra-alveolar eosinophils as well.

Discussion

The development of vaccines against emerging viruses can only begin from the moment the genetic code of the novel pathogen is known. From then a race against the

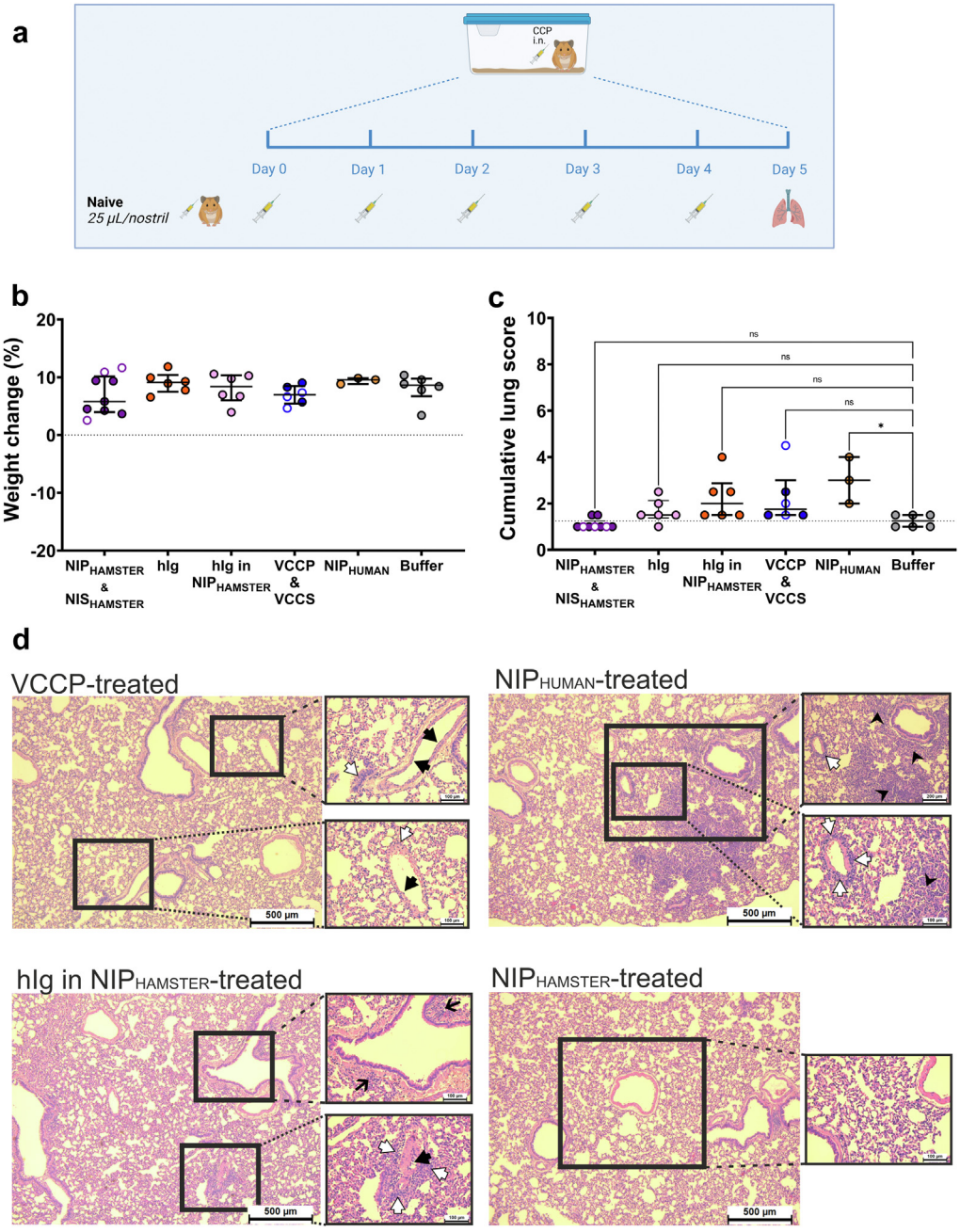

***Fig. 3:* Effects on the lung of hamsters treated i.n. with human versus hamster plasma in the absence of viral challenge.** (**a**) The study design depicts hamsters treated daily with hIg in $NIP_{HAMSTER}$ (n = 6), $NIP_{HAMSTER}$ (n = 3) and its derived serum (NIP_{SERUM}) (n = 3), hIg (n = 6), VCCP (n = 3) and its derived serum (VCCS) (n = 3), NIP_{HUMAN} (n = 3) or buffer (n = 6). (**b**) The relative weight change (%) determined on the day of sacrifice and normalized to that on day 0. (**c**) Cumulative lung score as determined by histopathologic assessment of H&E prepared lung sections. Statistical significance between cohorts was calculated by Kruskal–Wallis with Dunn's post hoc test. *P < 0.05, ns = not significant. (**b-c**) Individual dots represent biological repeats (*plasma,* ● & *serum,* ◯). Median (*horizontal line*) and interquartile range (*error bars*) are plotted. (**d**) Representative H&E-stained lung sections taken from a hamster that was treated i.n. with VCCP (*top left*), NIP_{HUMAN} (*top right*), hIg in $NIP_{HAMSTER}$ (*bottom left*) or $NIP_{HAMSTER}$ (*bottom right*). Inserts depict detailed sections, including some with specific signs of inflammation. Perivascular inflammation includes endothelialitis (*closed arrow,* ▲) and perivascular cuffs (*open arrow,* ⇧). Lung inflammation includes bronchopneumonia (*fine line arrow,* ↑) and pneumocyte hyperplasia (*butterfly arrow,* ⮝). Microscopic image acquisition was at 50 magnification (500 µm *scale bar*), using a 10×/20 objective with 5×/0.12 NA and bright field settings. Detailed images were acquired at 100 (200 µm *scale bar*) or 200 (100 µm *scale bar*) magnification, using a 10×/20 objective with 10×/0.22 NA or 20×/0.3 NA and bright field settings.

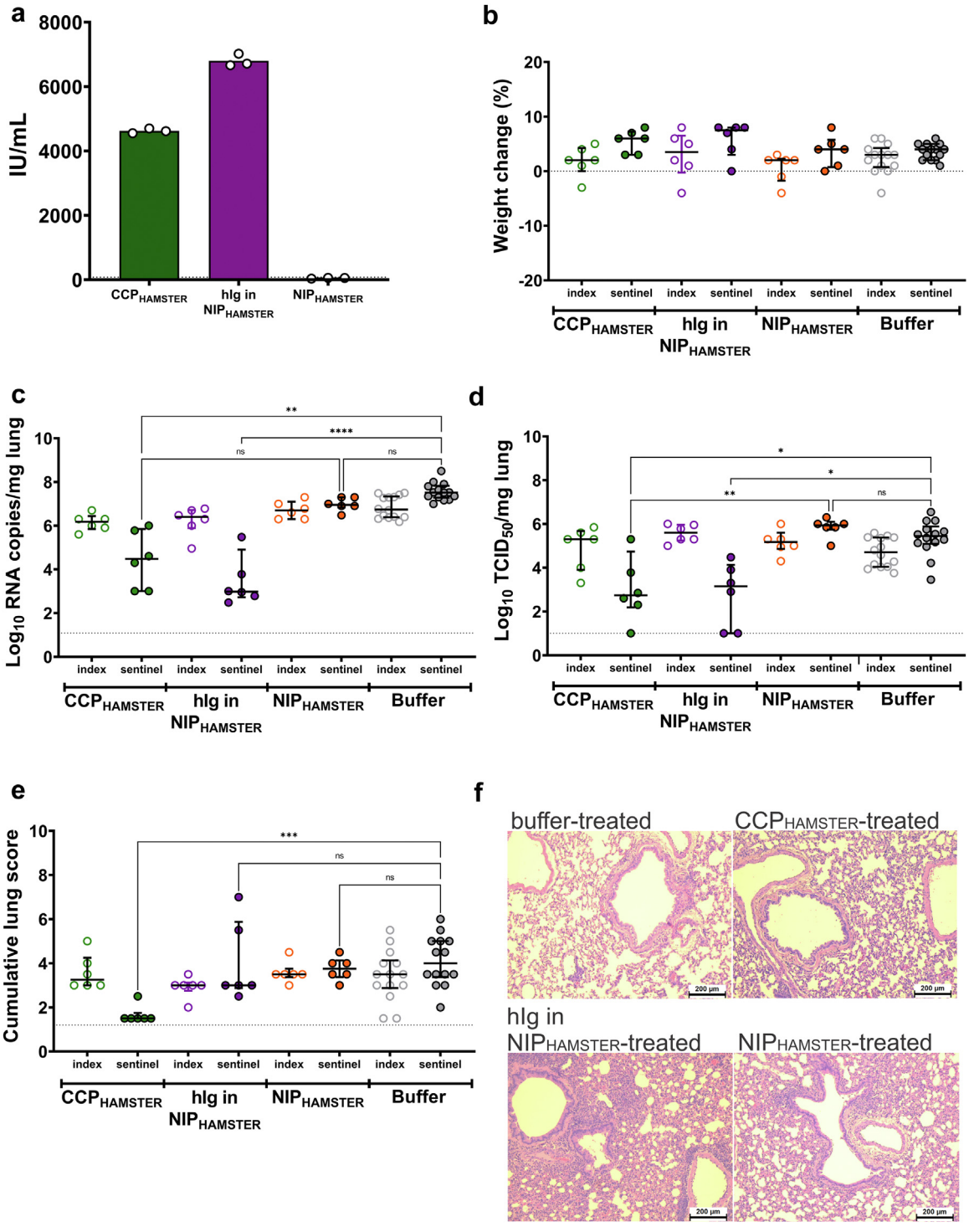

Fig. 4: **Intranasal administration of hamster (convalescent) plasma in hamsters as prophylaxis against SARS-CoV-2 transmission.** The study was designed as in Fig. 2a. Sentinel hamsters were treated daily from day 0 onwards with i.n. $CCP_{HAMSTER}$, hIg in $NIP_{HAMSTER}$, $NIP_{HAMSTER}$ (all n = 6) or buffer (n = 14) and index hamsters were inoculated at day 0 with SARS-CoV-2 ancestral strain. (**a**) Inhibition of ACE2 binding to RBD expressed as international WHO standard (IU/mL). Bars represent mean and dots individual data (technical repeats, n = 3). (**b**) The relative weight change (%) determined on the day of sacrifice and normalized to that on day 0. (**c**) Viral RNA levels in the lung measured by RT-qPCR and expressed as log_{10} genome copies/mg lung tissue. (**d**) Infectious virus in lung homogenate expressed as log_{10} $TCID_{50}$/mg lung tissue. (**e**) Cumulative lung score as

clock starts, as what followed after SARS-CoV-2 was described. In addition, broad spectrum antivirals against virus families with epidemic or pandemic potential are not available. Consequently, during an epi- or pandemic a first resort often is CP. Donor plasma is relatively inexpensive and is available from the moment an infected donor has recovered and has mounted a humoral immune response. First case studies with CCP transfusion in critically ill COVID-19 patients were reported in January 2020, one month after the first SARS-CoV-2 cases.[4] The first vaccines were available at breath-taking pace, but still took one year to reach the (Western) public.[31] Repurposed antivirals or monoclonal antibody (cocktails) were available in October 2020, with variable clinical efficacies.[32–35] This shows that other options for disease treatment and prevention are worthwhile investigating, especially for use early on in an epidemic.

Collection of plasma from donors that have recovered from COVID-19 is not different from regular plasma donation and is continuously operational in modern blood establishments. Hence, CP could be part of pandemic preparedness plans in no time. That is currently not the case because several trials suggest that CP transfusion is not efficacious by default[36] as was confirmed for COVID-19.[5–9]

Therefore, we investigated if CCP has potential as an intranasal prophylactic using a SARS-CoV-2 transmission model. We found a significant reduction in infectious virus in the lungs of 78% of treated hamsters, half of which had undetectable virus. When VCCP was used an even higher reduction was observed in all animals. The difference between CCP and VCCP is attributed to the 10-fold higher neutralizing titer following vaccination.[37,38] Regarding safety, i.n. treatment of hamsters with human CCP caused lung damage that was histologically different from the classical clinical picture of a SARS-CoV-2 infection in hamsters, characterized by pathological lung lesions, pulmonary edema, increased respiratory rate, decreasing activity and progressive weight loss reminiscent of the clinical picture in humans.[39,40] Instead, pneumocyte hyperplasia and intra-alveolar eosinophils was observed, a reactive (immune) response linked to the treatment. This characteristic histopathologic image was not observed when hamster CCP was used indicating a cross-species side effect.

Consistent with previous studies,[41] 20 μg/mL (130 nM) of anti-RBD IgG levels were detected in CCP compared to 100 μg/mL (670 nM) in VCCP. Treatment with VCCP prevented infection more than hIg. This difference may be caused by the presence of plasma matrix in VCCP or by higher IgA levels because the hIg sample had reduced IgA levels but retained the original IgG concentration. The latter fits with the basic immunologic finding that IgA is a prominent isotype in (nasal) mucosa.[42,43] Yet, the contribution of isotypes to the efficacy of i.n. prophylaxis requires further study.

If the hamster model translates to humans, i.n. administration of CCP may protect against transmission in the early days of a pandemic when little targeted therapy or prevention is available. We envision a naso-/oropharyngeal ("nasal") spray to protect the most vulnerable, i.e. elderly, patients with co-morbidities and health care workers. In addition, CCP nasal sprays may protect populations of low- and middle-income countries that have limited primary access to vaccines. In the general population, CCP nasal sprays may help in limiting the spread of disease even in vaccinated people who are now mostly protected from hospitalization but not from infection.

Because CCP availability is crucial to provide a potential nasal spray to (sub)populations, we estimated the balance of supply and demand using Belgian healthcare data. In Belgium, the first epidemic COVID-19 'wave' started in March 2020. At the end of April, 5% of Belgian blood donors was positive for anti-SARS-CoV-2 antibodies, representing 12,500 (known) donors. Four months later, a second wave hit the country causing 7500 hospital admissions significantly straining the healthcare system.[44,45] Assuming these hospitalized COVID-19 cases were all 'vulnerable' *a priori* and that this population could be identified in May based on healthcare records, supplying them with a CCP nasal spray for twice daily use (200 μL/nostril) in September for 200 consecutive days (i.e. winter season) would have required 1200 L of CCP. This implies the need for 2400 successful CCP donations starting from May 2020. Having 12,500 potential donors from the first wave and a logistic machine that deals with 200,000 plasma donations per year, this should have been feasible.

However, the efficacy of CCP sourced from donors infected with the ancestral strain will be decreasing over time. Consistent with other studies,[30] our data suggest that Delta and Omicron variants are still inhibited by CCP sourced from convalescent donors infected with the ancestral strain but with a respective

determined by histopathologic assessment of H&E prepared lung sections (**b-e**) Individual dots represent biological repeats. The median (*horizontal line*) and interquartile range (*error bars*) are plotted. The horizontal dotted line represents the lower limit of detection. Statistical significance between cohorts was calculated by Kruskal–Wallis with Dunn's post hoc test. *P < 0.05, **P < 0.01, ***P < 0.001, ****P < 0.0001, ns = not significant. Individual data are plotted with median (*horizontal line*) and interquartile range (*error bars*). (**f**) Representative H&E-stained lung sections taken from a sentinel hamster that treated i.n. with buffer (*top left*), $CCP_{HAMSTER}$ (*top right*), hIg in $NIP_{HAMSTER}$ (*bottom left*) or $NIP_{HAMSTER}$ (*bottom right*). Microscopic image acquisition was at 100 magnification (200 μm *scale bar*), using a 10×/20 objective with 10×/0.22 NA and bright field settings.

decrease of 2- and 5-fold by $PRNT_{50}$. Because plasma donation is a common activity in many high-income countries, a continuous supply of CCP maximally adapted to the recent virus strains is not impossible. This will require performant and adaptive laboratory tests to allow continuous monitoring of the donor population.[46–48]

Limitations of this study are the restrictions in translating the *in vivo* animal model studies to humans and the identification of the mechanism of action. Because hamsters are obligatory nasal breathers, part of the administered CCP will reach the lungs which is evident from the lung reactions to allogeneic human plasma. Consequently, the antiviral effect of i.n. delivered CCP requires topological discrimination between upper and lower airways.

Future epidemics or pandemics are best tackled using prophylactics like vaccines as soon as these are available. This assumes effective vaccines can be developed at all, which is not always the case as is seen with HIV. Our study now suggests that for SARS-CoV-2 and possibly for other airborne pathogens, CP may be developed in a similar way, i.e. for prophylaxis. Because airborne viruses primarily infect respiratory and oral mucosae,[49] fighting inhaled viruses at the exact place of initial infection using CP may have profound implications for future epidemic management.

Contributors

VC, HBF and EW coordinated the study. HBF, EW, CV and RA designed the study. EW, CV, RA, RD and BW performed laboratory experiments and data collection. EW, CV and HBF verified the underlying data. BW performed lung scoring. DDC coordinated donor recruitment. DJ coordinated PRNT screening. DDB performed biobanking operations. EW, CV, VC, JN and HBF performed data interpretation. CV performed statistical analysis. EW, CV and HBF drafted the manuscript. All authors read and approved (the submission of) the final manuscript.

Data sharing statement

All analysed data generated during this study are included in this published article. Individual histopathology scoring data can be found in a data supplement available with the online version of this article. Raw data can be made available by the corresponding author upon request.

Declaration of interests

Hendrik B. Feys and Veerle Compernolle are listed as inventors on a patent priority application (22199947.7.A) on this subject. The remaining authors declare no conflict of interest.

Acknowledgements

We thank all donors who have voluntarily donated (convalescent) plasma and who consented to using parts of their donation for scientific research. We thank the many Belgian Red Cross Flanders employees who have participated in donor recruitment, plasma collection, component manufacturing, CCP (sample) distribution and quality assessment during the pandemic. We thank Sabrina Seghers for her contributions to biobank operations. We thank Carolien De Keyzer and Lindsey Bervoets for their contributions in the *in vivo* hamster studies. This study was funded by Flanders Innovation & Entrepreneurship (VLAIO) and the Foundation for Scientific Research of the Belgian Red Cross Flanders. Figs. 2a and 3a were created in BioRender.com.

Appendix A. Supplementary data

Supplementary data related to this article can be found at https://doi.org/10.1016/j.ebiom.2023.104597.

References

1 Hassani A, Khan G. Human-animal interaction and the emergence of SARS-CoV-2. *JMIR Public Health Surveill*. 2020;6(4):e22117.
2 Jones KE, Patel NG, Levy MA, et al. Global trends in emerging infectious diseases. *Nature*. 2008;451(7181):990–993.
3 Berkley S. Even after COVID, the world's vaccine strategy is failing. *Nature*. 2022;612:377.
4 Shen C, Wang Z, Zhao F, et al. Treatment of 5 critically ill patients with COVID-19 with convalescent plasma. *JAMA*. 2020;323(16):1582–1589.
5 Abani O, Abbas A, Abbas F, et al. Convalescent plasma in patients admitted to hospital with COVID-19 (RECOVERY): a randomised controlled, open-label, platform trial. *Lancet*. 2021;397(10289):2049–2059.
6 Devos T, Van Thillo Q, Compernolle V, et al. Early high antibody-titre convalescent plasma for hospitalised COVID-19 patients: DAWn-plasma. *Eur Respir J*. 2021;59(2):2101724.
7 Korley FK, Durkalski-Mauldin V, Yeatts SD, et al. Early convalescent plasma for high-risk outpatients with Covid-19. *N Engl J Med*. 2021;385(21):1951–1960.
8 Estcourt LJ. Passive immune therapies: another tool against COVID-19. *Hematology Am Soc Hematol Educ Program*. 2021;2021(1):628–641.
9 Investigators TR-C, Estcourt LJ. Convalescent plasma in critically ill patients with Covid-19. *medRxiv*. 2021. https://doi.org/10.1101/2021.06.11.21258760.
10 Betrains A, Godinas L, Woei AJF, et al. Convalescent plasma treatment of persistent severe acute respiratory syndrome coronavirus-2 (SARS-CoV-2) infection in patients with lymphoma with impaired humoral immunity and lack of neutralising antibodies. *Br J Haematol*. 2021;192(6):1100–1105.
11 Hueso T, Godron AS, Lanoy E, et al. Convalescent plasma improves overall survival in patients with B-cell lymphoid malignancy and COVID-19: a longitudinal cohort and propensity score analysis. *Leukemia*. 2022;36(4):1025–1034.
12 Sullivan DJ, Gebo KA, Shoham S, et al. Early outpatient treatment for Covid-19 with convalescent plasma. *N Engl J Med*. 2022;386(18):1700–1711.
13 Tworek A, Jaron K, Uszynska-Kaluza B, et al. Convalescent plasma treatment is associated with lower mortality and better outcomes in high-risk COVID-19 patients - propensity-score matched case-control study. *Int J Infect Dis*. 2021;105:209–215.
14 Levine AC, Fukuta Y, Huaman MA, et al. COVID-19 convalescent plasma outpatient therapy to prevent outpatient hospitalization: a meta-analysis of individual participant data from five randomized trials. *Clin Infect Dis*. 2023:ciad088.
15 Senefeld JW, Franchini M, Mengoli C, et al. COVID-19 convalescent plasma for the treatment of immunocompromised patients: a systematic review and meta-analysis. *JAMA Netw Open*. 2023;6(1):e2250647.
16 Senefeld JW, Gorman EK, Johnson PW, et al. Mortality rates among hospitalized patients with COVID-19 treated with convalescent plasma A Systematic review and meta-analysis. *medRxiv*. 2023. https://doi.org/10.1101/2023.01.11.23284347.
17 Hou YJ, Okuda K, Edwards CE, et al. SARS-CoV-2 reverse genetics reveals a variable infection gradient in the respiratory tract. *Cell*. 2020;182(2):429–446.e14.
18 Sungnak W, Huang N, Becavin C, et al. SARS-CoV-2 entry factors are highly expressed in nasal epithelial cells together with innate immune genes. *Nat Med*. 2020;26(5):681–687.
19 Ziegler CGK, Allon SJ, Nyquist SK, et al. SARS-CoV-2 receptor ACE2 is an interferon-stimulated gene in human airway epithelial cells and is detected in specific cell subsets across tissues. *Cell*. 2020;181(5):1016–1035.e19.
20 Mouro V, Fischer A. Dealing with a mucosal viral pandemic: lessons from COVID-19 vaccines. *Mucosal Immunol*. 2022;15(4):584–594.
21 Kristiansen PA, Page M, Bernasconi V, et al. WHO International Standard for anti-SARS-CoV-2 immunoglobulin. *Lancet*. 2021;397(10282):1347–1348.
22 Wouters E, Verbrugghe C, Devloo R, et al. A novel competition ELISA for the rapid quantification of SARS-CoV-2 neutralizing

antibodies in convalescent plasma. *Transfusion*. 2021;61(10):2981–2990.
23 Spiteri G, Fielding J, Diercke M, et al. First cases of coronavirus disease 2019 (COVID-19) in the WHO European region, 24 January to 21 February 2020. *Euro Surveill*. 2020;25(9):2000178.
24 Park YJ, De Marco A, Starr TN, et al. Antibody-mediated broad sarbecovirus neutralization through ACE2 molecular mimicry. *Science*. 2022;375(6579):449–454.
25 Imbrechts M, Maes W, Ampofo L, et al. Potent neutralizing anti-SARS-CoV-2 human antibodies cure infection with SARS-CoV-2 variants in hamster model. *iScience*. 2022;25(8):104705.
26 Abdelnabi R, Foo CS, Zhang X, et al. The omicron (B.1.1.529) SARS-CoV-2 variant of concern does not readily infect Syrian hamsters. *Antiviral Res*. 2022;198:105253.
27 Kaptein SJF, Jacobs S, Langendries L, et al. Favipiravir at high doses has potent antiviral activity in SARS-CoV-2-infected hamsters, whereas hydroxychloroquine lacks activity. *Proc Natl Acad Sci U S A*. 2020;117(43):26955–26965.
28 Reed LJ, Muench H. A simple method of estimating fifty per cent ENDPOINTS12. *Am J Epidemiol*. 1938;27(3):493–497.
29 Boudewijns R, Thibaut HJ, Kaptein SJF, et al. STAT2 signaling restricts viral dissemination but drives severe pneumonia in SARS-CoV-2 infected hamsters. *Nat Commun*. 2020;11(1):5838.
30 Wang Y, Ma Y, Xu Y, et al. Resistance of SARS-CoV-2 Omicron variant to convalescent and CoronaVac vaccine plasma. *Emerg Microbes Infect*. 2022;11(1):424–427.
31 Fauci AS. The story behind COVID-19 vaccines. *Science*. 2021;372(6538):109.
32 WHO Solidarity Trial Consortium, Pan H, Peto R, et al. Repurposed antiviral drugs for Covid-19 - interim WHO solidarity trial results. *N Engl J Med*. 2021;384(6):497–511.
33 Fischer WA 2nd, Eron JJ Jr, Holman W, et al. A phase 2a clinical trial of molnupiravir in patients with COVID-19 shows accelerated SARS-CoV-2 RNA clearance and elimination of infectious virus. *Sci Transl Med*. 2022;14(628):eabl7430.
34 Loo YM, McTamney PM, Arends RH, et al. The SARS-CoV-2 monoclonal antibody combination, AZD7442, is protective in nonhuman primates and has an extended half-life in humans. *Sci Transl Med*. 2022;14(635):eabl8124.
35 Levin MJ, Ustianowski A, De Wit S, et al. Intramuscular AZD7442 (Tixagevimab-Cilgavimab) for prevention of Covid-19. *N Engl J Med*. 2022;386(23):2188–2200.
36 van Griensven J, Edwards T, de Lamballerie X, et al. Evaluation of convalescent plasma for Ebola virus disease in Guinea. *N Engl J Med*. 2016;374(1):33–42.
37 Carreno JM, Alshammary H, Tcheou J, et al. Activity of convalescent and vaccine serum against SARS-CoV-2 Omicron. *Nature*. 2022;602(7898):682–688.
38 Kuzmina A, Khalaila Y, Voloshin O, et al. SARS-CoV-2 spike variants exhibit differential infectivity and neutralization resistance to convalescent or post-vaccination sera. *Cell Host Microbe*. 2021;29(4):522–528.e2.
39 Imai M, Iwatsuki-Horimoto K, Hatta M, et al. Syrian hamsters as a small animal model for SARS-CoV-2 infection and countermeasure development. *Proc Natl Acad Sci U S A*. 2020;117(28):16587–16595.
40 Rosenke K, Meade-White K, Letko M, et al. Defining the Syrian hamster as a highly susceptible preclinical model for SARS-CoV-2 infection. *Emerg Microbes Infect*. 2020;9(1):2673–2684.
41 Ma H, Zeng W, He H, et al. Serum IgA, IgM, and IgG responses in COVID-19. *Cell Mol Immunol*. 2020;17(7):773–775.
42 Russell MW, Moldoveanu Z, Ogra PL, Mestecky J. Mucosal immunity in COVID-19: a neglected but critical aspect of SARS-CoV-2 infection. *Front Immunol*. 2020;11:611337.
43 Smith N, Goncalves P, Charbit B, et al. Distinct systemic and mucosal immune responses during acute SARS-CoV-2 infection. *Nat Immunol*. 2021;22(11):1428–1439.
44 Bruyneel A, Gallani MC, Tack J, et al. Impact of COVID-19 on nursing time in intensive care units in Belgium. *Intensive Crit Care Nurs*. 2021;62:102967.
45 de Pelsemaeker MC, Guiot Y, Vanderveken J, Galant C, Van Bockstal MR. The impact of the COVID-19 pandemic and the associated Belgian governmental measures on Cancer screening, surgical Pathology and Cytopathology. *Pathobiology*. 2021;88(1):46–55.
46 Wouters E, Steenhuis M, Schrezenmeier H, et al. Evaluation of SARS-CoV-2 antibody titers and potency for convalescent plasma donation: a brief commentary. *Vox Sang*. 2021;116(5):493–496.
47 Nguyen D, Simmonds P, Steenhuis M, et al. SARS-CoV-2 neutralising antibody testing in Europe: towards harmonisation of neutralising antibody titres for better use of convalescent plasma and comparability of trial data. *Euro Surveill*. 2021;26(27):2100568.
48 Focosi D, Franchini M, Joyner MJ, Casadevall A. Are convalescent plasma stocks collected during former COVID-19 waves still effective against current SARS-CoV-2 variants? *Vox Sang*. 2022;117(5):641–646.
49 Ghosh S, Kumar M, Santiana M, et al. Enteric viruses replicate in salivary glands and infect through saliva. *Nature*. 2022;607(7918):345–350.